In Situ Diamond-Anvil Cell Observations of Methanogenesis at High Pressures and Temperatures

ARTICLE *in* ENERGY & FUELS · NOVEMBER 2009

Impact Factor: 2.79 · DOI: 10.1021/ef9006017

3 AUTHORS, INCLUDING:

Anurag Sharma
Suffolk University
21 PUBLICATIONS **708** CITATIONS

SEE PROFILE

Russell J Hemley
Carnegie Institution for Science
789 PUBLICATIONS **25,656** CITATIONS

SEE PROFILE

Energy Fuels **XXXX,** *XXX,* 000–000 · DOI:10.1021/ef9006017

energy&fuels
article

In Situ Diamond-Anvil Cell Observations of Methanogenesis at High Pressures and Temperatures

Anurag Sharma,* George D. Cody, and Russell J. Hemley

Geophysical Laboratory, Carnegie Institution of Washington, 5251 Broad Branch Road, Northwest, Washington, District of Columbia 20015

Received June 12, 2009. Revised Manuscript Received September 8, 2009

In situ high pressure−temperature ($P-T$) measurements on C−H−O fluids at lower crust and upper mantle conditions have been performed to assess the extent and limit of methane generation within the Earth. Experiments were conducted using diamond-anvil cells at temperatures from 250 to >1500 °C and pressures between 1 and 8 GPa, assuming conditions along a subduction-setting geotherm. In many experiments, methanogenesis is observed, in particular, in those experiments in which elemental carbon or reduced transition metals (e.g., Fe^0) were present. The direct reduction of CO_2 to methane was not observed under any set of conditions. Methanogenesis is sensitive to C−H−O fluid composition and, specifically, the activity of H_2. Kinetic barriers to direct hydrogenation of CO persists over the range of conditions explored, and hydrogenated transition-metal carbonyl species likely play a critical role in methane formation. Surprisingly, the direct hydrogenation of graphite yields considerable methane. The observation of both CO_2 and H_2 generation during high T and P reactions of ferrous oxide, calcium carbonate, and water indicates that methanogenesis in the lower crust and upper mantle is plausible; however, the absolute yield of methane is strongly controlled by the activity of H_2.

1. Introduction

The conversion of C1 oxides (CO and possibly CO_2) and H_2 into hydrocarbons was first demonstrated over a century ago and continues to be used as an industrially viable means of conversion of coal (albeit indirectly via initial conversion to syn-gas, $CO + H_2$) into hydrocarbon fuels.[1] The mechanistic details of such chemistry, broadly referred to as the Fischer−Tropsch-type (FTT) process, have been extensively studied.[1,2] From a thermodynamic standpoint, reduction of CO_x with H_2 to CH_4 is favored at lower temperatures but is kinetically inhibited and thus requires catalysts. It is also well-established that high pressures (industrially in the range of 35 MPa) enhance carbon chain growth, favoring the synthesis of liquid over gaseous hydrocarbons.[2] From an industrial perspective, the FTT process is mature chemistry and advances have focused on developing better catalysts rather than more severe reaction conditions to enhance the cost effectiveness relative to that of extracting and refining biologically derived petroleum liquids.

Notwithstanding the relative antiquity of industrial FTT chemistry, only over the past couple of decades has the possibility that FTT chemistry may have occurred naturally as a consequence of CO_2 and H_2 reactions within the Earth's crust and perhaps even the mantle been taken seriously by the geochemical community. Speculation that hydrocarbon synthesis could occur in deep Earth environments dates back to at least the early 19th century when Mendeleev proposed an abiotic origin for petroleum observed along deep fractures.[3]

The potential for deep Earth hydrocarbon generation is suggested by the continuous cycling of carbon and water into the mantle as a consequence of the subduction alteration of the oceanic seafloor. There does not exist an accurate assessment of the efficiency by which carbon and water are delivered to the deep mantle as opposed to being lost because of decarbonation and dehydration into the overlying mantle wedge. The activity of carbon in certain regions of the mantle is high enough to lead to the formation of diamond, carbonatite magma, and other carbon-bearing phases.[4] Intriguing low seismic velocity zones detected tomographically exist within the mantle and may indicate the presence of water and other volatile phases.[5] Some evidence that abiogenic hydrocarbon synthesis occurs at least on a small scale was shown recently using compound-specific hydrogen isotopic analysis of hydrocarbon gases emanating from fractured granite associated with the Kidd Creek mine, Canada.[6] However, such observations remain scarce and have been limited to the accessible shallow crust. The possibility of massive mantle hydrocarbon generation has been promoted extensively by a small group of proponents,[7−9] but many questions remain

*To whom correspondence should be addressed. Telephone: 202-478-7975. Fax: 202-478-8901. E-mail: asharma@ciw.edu.

(1) Anderson, R. B. *The Fischer−Tropsch Synthesis*; Academic Press: Orlando, FL, 1984.
(2) Davis, B. H.; Occelli, M. L. *Fischer−Tropsch Syntesis, Catalysts and Catalysis*; Elsevier BV: Amsterdam, The Netherlands, 2007.
(3) Mendeleef, M. L'origine du petrole. *Rev. Sci.* **1877**, *13*, 409–416.
(4) Haggerty, S. A diamond trilogy: Superplumes, supercontinents, and supernovae. *Science* **1999**, *285*, 851–860.
(5) Anderson, D. L. *A New Theory of Earth*; Cambridge University Press: Cambridge, U.K., 2007.
(6) Westgate, T. D.; Ward, J. A.; Slater, G. F.; Lacrampe-Couloume, G.; Sherwood Lollar, B. Abiogenic formation of alkanes in the Earth's crust as a minor source for global hydrocarbon reservoirs. *Nature* **2002**, *416*, 522–524.
(7) Gold, T. The deep, hot biosphere. *Proc. Natl. Acad. Sci. U.S.A.* **1992**, *89*, 6045–6049.
(8) Gold, T. *The Deep Hot Bioshpere*; Copernicus: New York, 1999.
(9) Kudryavtsev, N. A. *Oil and Gas Origin*; Nedra: Moscow, Russia, 1973.

concerning the feasibility of formation and stability of hydrocarbons in the deep Earth.[10]

The extent to which hydrocarbons constitute a thermodynamically stable phase at upper mantle conditions has been the focus of discussion since the earliest conjectures of deep oil and gas. A case for thermodynamic stability was put forth by Kenney et al.[11] based on thermodynamic arguments and high $P-T$ experiments ($T > 1000$ °C and P at 4−5 GPa).[11] These experiments focused on the reaction of ferrous oxide, calcium carbonate, and water, in a large volume rapid-quench high-pressure device that enabled mass spectroscopic analysis of the extracted hydrocarbon phases; methane and higher hydrocarbons were detected. Subsequently, this chemical system was investigated by Scott et al.,[12] who used diamond-anvil cell (DAC) methods that allowed for *in situ* Raman spectroscopy of fluids and X-ray diffraction characterization of the solid phases at upper mantle $P-T$ conditions (500−1500 °C and 5−11 GPa). Scott et al.[12] noted that methane formation was favored at lower temperatures, whereas Kenney et al.[11] suggested that methane yield increased continuously from 700 to near 1200 °C. Thermodynamic calculations by Scott et al.[12] suggested that methane should not in fact be a stable species at temperatures as high as 1500 °C. Both experimental studies demonstrated the formation of methane at high $P-T$ conditions and have opened up a series of new questions about relative roles of thermodynamic and kinetic control of the reactions and the effects of pressure, temperature, and composition over a wider range of conditions. In addition, the possible role of reduced transition metals from the reactor walls in affecting hydrocarbon synthesis reactions[13] needs to be examined. For example, if the reactor wall material becomes a reactant, the incorporation of reduced metals in the system will increase the hydrogen fugacity of the system.

In the present study, the problem of CO_2 reduction to hydrocarbons (methane and higher homologues) is investigated further using DACs and *in situ* Raman spectroscopy. We explore the extent of reduced metal participation in hydrocarbon synthesis reactions and re-investigate the ferrous oxide−calcium carbonate−water reaction and the role of a pure carbon-bearing phase (graphite) that has been postulated to enhance the thermodynamic stability of hydrocarbons at elevated $P-T$ conditions.

2. Experimental Section

DAC devices generates high pressures and temperatures while providing a direct window to samples for *in situ* observations and measurements under extreme conditions.[14] This study used modified DACs mounted typically with a pair of anvils having 800 μm culets that compress samples combined within 300−500 μm diameter and 100−250 μm sample chambers formed by metal gaskets.[15] The circular sample chambers were also typically lined with 10−20 μm annulus of gold foil to block possible reactions between the sample and the bulk of the gasket (usually rhenium).[16] A pair of nichrome resistive heaters mounted at the base of the two anvils was capable of heating the DAC rapidly up to 1000 °C (Figure 1).[15] The temperature was measured with an accuracy of ±5 °C using a pair of thermocouples glued directly on the anvils on either side of the sample chamber. Pressure within the sample cavity was measured by the calibrated pressure-induced shift in the fluorescence spectrum of a ruby chip placed within the cavity.[17,18] At high temperatures where ruby fluorescence is weak, the pressure was determined from well-established pressure induced Raman vibrational frequency shifts of various phases present in the system (diamond, CO_2, CH_4, and H_2), yielding a precision of ±0.5 GPa.[17,19,20] For experiments conducted at higher temperatures (>1000 °C), a continuous-wave 60 W Nd:YAG near-infrared laser (1.06 μm) was used as the heating source. Thermal gradients because of a relatively small laser heating spot (<30 μm) make the temperature determination less precise.[14] Such experiments were performed only to test the feasibility of methane formation at high $P-T$ conditions and were limited to graphite−hydrogen interactions.

A typical experimental protocol involved pressurizing the sample to a specific pressure at room temperature (cold pressure). Upon heating, the thermal expansion of the sample typically resulted in a pressure increase relative to the initial pressure, an effect that depended upon the temperature.[15] Sample loadings were performed with care not to introduce contaminants into the sample chamber. The diamond surfaces were thoroughly cleaned with several washes of doubly distilled deionized water and avoiding any use of organic solvents, whereas the gasket was first cleaned in an ultrasonic bath in deionized distilled water and then placed on the diamond surface for immediate loading. High-purity (>99%) solid phases (i.e., Fe−oxides, carbonates, and Fe/Ni nanopowder) were obtained from Alfa Aesar and were introduced in the chamber first, followed by the aqueous phase that included formic acid (99% purity from Acros Organics), used as a source of CO_2 and H_2. The aqueous phase was loaded to completely fill the sample chamber; i.e., there was no headspace (no vapor bubble) when the cell was closed for compression. Once loaded, the DAC was immediately taken to the desired high cold pressure ($P_{initial}$) at ambient temperature and set for subsequent heating (Figure 1 and Table 1). The resistive heating rates were typically 100 °C/min until the desired temperature was reached and maintained for at least $^1/_2$ h, while *in situ* optical measurements were performed. Hydrogen, for the laser heating experiments, was loaded in DACs as a gas at room temperature inside a custom-built high-pressure vessel and at ∼200 MPa using this technique; the DAC is opened and then closed remotely to trap the hydrogen in the sample chamber.[21]

(10) Glazby, G. P. Abiotic origins of hydrocarbons: An historical review. *Resour. Geol.* **2006**, *56*, 85–98.
(11) Kenney, J. F.; Kutcherov, V. A.; Bendeliani, N. A.; Alekseev, V. A. The evolution of multicomponent systems at high pressures: VI. The thermodynamic stability of the hydrogen−carbon system: The genesis of hydrocarbons and the origin of petroleum. *Proc. Nat. Acad. Sci. U.S.A.* **2002**, *99*, 10976–10981.
(12) Scott, H. P.; Hemley, R. J.; Mao, H. K.; Herschbach, D. R.; Fried, L. E.; Howard, W. M.; Bastea, S. Generation of methane in the Earth's mantle: In-situ high $P-T$ measurements of carbonate reduction. *Proc. Nat. Acad. Sci. U.S.A.* **2004**, *101*, 14023–14026.
(13) Maiella, P. G.; Brill, T. B. Spectroscopy of hydrothermal reactions. 10. Evidence of wall effects and decarboxylation kinetics of 1.00 m HCO_2X (X = H, Na) at 280−330 °C and 275 bar. *J. Phys. Chem. A* **1998**, *102*, 5886–5891.
(14) Hemley, R. J.; Mao, H. K. New windows on earth and planetary interiors. *Mineral. Mag.* **2002**, *66*, 791–811.
(15) Bassett, W. A.; Shen, A. H.; Bucknum, M.; Chou, I. M. A new diamond anvil cell for hydrothermal studies to 2.5 GPa and from −190 to 1200 °C. *Rev. Sci. Instrum.* **1993**, *64*, 2340–2345.
(16) Sharma, A.; Cody, G. D.; Scott, J.; Hemley, R. J., Molecules to microbes: In-situ studies of organic systems under hydrothermal conditions. In *Chemistry under Extreme Conditions*; Manaa, R., Ed.; Elsevier Science: Amsterdam, The Netherlands, 2005.
(17) Goncharov, A. F.; Zaug, J. M.; Crowhurst, J. C. Optical calibration of pressure sensors for high pressures and temperatures. *J. Appl. Phys.* **2005**, *97*, No. 094917.
(18) Mao, H. K.; Bell, P. M.; Shaner, J. W.; Steinberg, D. J. Specific volume measurements of Cu, Mo, Pd, and Ag and calibration of the ruby R1 fluorescence pressure gauge from 0.06 to 1 Mbar. *J. Appl. Phys.* **1978**, *49*, 3276.
(19) Tardieu, A.; Cansell, F.; Petitet, J. P. Pressure and temperature dependence of first-order Raman mode of diamond. *J. Appl. Phys.* **1990**, *68*, 3243–3245.
(20) Hemley, R. J. Effects of high pressure on molecules. *Annu. Rev. Phys. Chem.* **2000**, *51*, 763–800.
(21) Somayazulu, M.; Finger, L. W.; Hemley, R. J.; Mao, H. K. High-pressure compounds in methane−hydrogen mixtures. *Science* **1996**, *271*, 1400–1402.

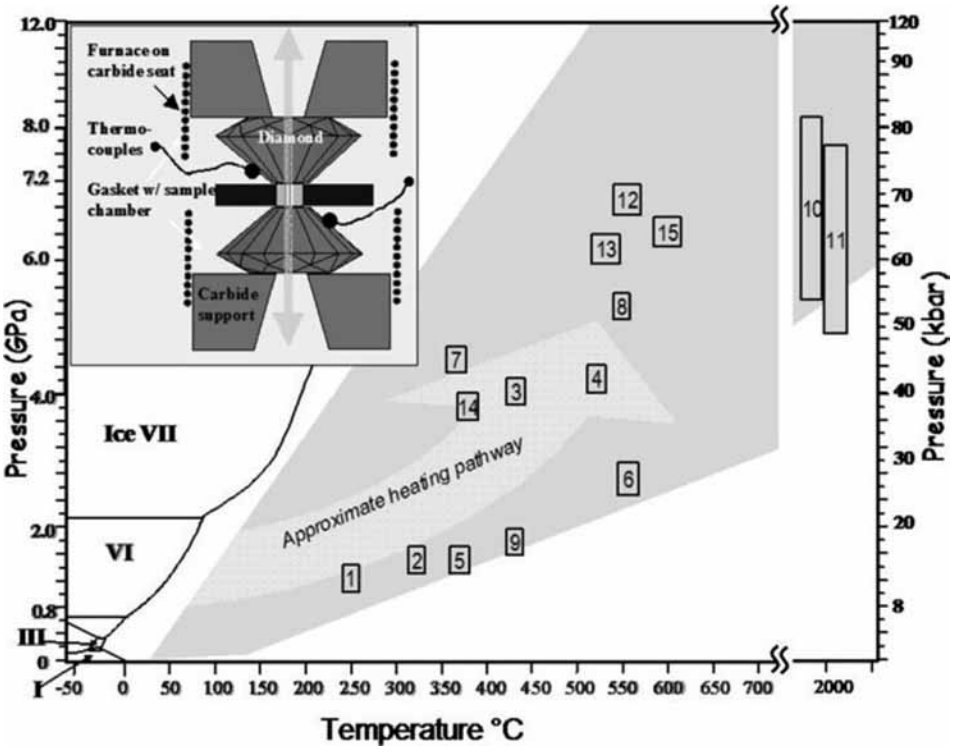

Figure 1. Schematic representation of the experimental conditions considered here for abiogenic formation of hydrocarbon. Most experiments were initiated near ~1.0 GPa; however, at high temperature, higher pressures were typically achieved and, in some cases, also manually adjusted to maintain conditions within an estimated geothermal gradient (shown above as a dark gray region). The numbers shown in the figure designate experimental conditions that correspond to individual experiments in Table 1. The inset shows a schematic of the DAC setup with external resistive heaters used for achieving high temperatures under pressure. The diamonds allow optical access to the entire sample while keeping the system under fixed pressure.

Table 1. Experiment Description and Results

run number (refer to Figure 1)	starting material	reactor	conditions (highest T, P)	products[a] CH_4	CO_2	CO	H_2	H_2O	other
1	pure formic acid	Au lined	330 °C, 1.2 GPa	n/d	s	s	s	s	n/d
2	pure formic acid	Au lined	550 °C, 5.5 GPa	n/d	s	s	s	s	n/d
3	pure formic acid	stainless steel	250 °C, 1.0 GPa	m	w	s	s	s	Fe−carbonate, $Fe(CO)_x$
4	pure formic acid, Fe nanoparticles	Au lined	440 °C, 1.5 GPa	m	w	s	m	m	Fe−carbonate, $Fe(CO)_x$
5	pure formic acid, FeO nanoparticles	Au lined	560 °C, 3.5 GPa	s	m	s	w	s	Fe−carbonate, $Fe(CO)_x$
6	CO_2, H_2O, FeO, Fe nanoparticles	Au lined	360 °C, 2.5 GPa	m	m/w	s	m	m	CO_2, Fe−carbonate, CO, H_2 no detectable C−H
7	graphite−formic acid	Au lined	350 °C, 4.5 GPa	s	s	w	m	m	graphite
8	graphite−formic acid	Cu−Be	420 °C, 4.0 GPa	s	s	m	m	m	graphite
9	graphite−formic acid	Au lined	550 °C, 4.5 GPa	s	s	m	m	m	C−H, more than methane
10	graphite−H_2	Au lined	>1500 °C, 5.5 GPa	s	n/d	n/d	s	n/d	graphite
11	graphite−H_2	rhenium	>1500 °C, 5.0 GPa	s	n/d	n/d	s	n/d	graphite
12	FeO−$CaCO_3$−H_2O +Fe nanopowder	Au lined	550 °C, 7.0 GPa	m	w	s	m	s	Fe−carbonyl, Fe/Ca−carbonate
13	FeO−$CaCO_3$−H_2O	stainless steel	520 °C, 6 GPa	m	m	s	m	s	Fe−carbonyl, Fe/Ca−carbonate
14	FeO−$CaCO_3$−H_2O	Au lined	350 °C, 4.0 GPa	n/d	s	w	w	s	Fe/Ca−carbonate, Fe−oxides
15	FeO−$CaCO_3$−H_2O	Au lined	620 °C, 6.5 GPa	w	s	w	w	s	Fe/Ca−carbonate, magnetite

[a] s, strong; m, moderate; w, weak; vw, very weak; n/d, not detected.

Molecular species were identified at high $P-T$ conditions in the DACs using Raman spectroscopy complemented by optical microscopy. Laser excitation wavelengths included 632, 540, 514.5, and 488 nm, which were selected to minimize fluorescence and possible laser damage to the sample. Several spectrometers equipped with multiple grating monochromators and CCD detectors were used to record the spectra. Typically, low-resolution measurements (300 lines/mm grating) were supplemented with high-resolution measurements (1500 lines/mm grating) in spectral regions of interest. Because of shifts and possible changes in the cross-section of Raman peaks at high $P-T$ conditions, quantitative determination of phase abundances was not possible without considerable standardization. However, it is straightforward to monitor changes in the relative peak areas of co-existing species to provide information on the extent of a given reaction.

3. Results and Discussion

3.1. CO_2-H_2 Reactions through Formic Acid Decomposition. Pure formic acid was loaded in the DAC and taken to

high temperatures (> 350 °C) to fully decompose at moderate to low pressures (< 0.5 GPa), yielding a mixture of CO_2, CO, H_2O, and H_2, consistent with previous work.[22−26] This system was then adjusted to the desired run $P-T$ conditions (250−550 °C and 1−5 GPa, runs 1, 2, and 3 in Table 1). The fluid composition is assumed to be fixed by the water−gas shift (WGS) equilibrium. Several experiments were performed with Au-lined reactors to avoid any participation of transition metals derived from the reactor surface (e.g., runs 1 and 2 in Table 1). In these experiments, microscopic observations reveal immiscible liquid phases (up to at least 400 °C along the $P-T$ path), one of which upon quenching solidifies into a crystalline phase. Raman analysis of the fluid phase that solidifies reveals a single CO-stretch peak (2100−2200 cm^{-1}) at high temperatures (Figure 2); the quenched solid phase reveals peak broadening, indicating clathrate formation upon quenching.[27,28] Consistent with previous work on C−H−O fluids sealed in silica tubes,[29] *in situ* Raman measurements reveal only peaks associated with CO_2, CO, H_2O, and H_2 (Figure 2); there is no detectable methane despite the fact that some methane would be expected on the basis of thermodynamic considerations, which suggests the persistence of kinetic barriers to methane formation.

The WGS equilibrium is maintained in these experiments over repeated $P-T$ cycling (over a period of several days) with no indication of hydrocarbon formation within the $P-T$ range described above. Changing $P-T$ conditions of the system alters the chemical equilibrium that is reflected in the proportionate change in the fluid composition, as monitored by *in situ* Raman spectroscopy (Figures 2 and 3). To quantitate molecular speciation within the fluid phases with temperature and pressure, relative distribution ratios are determined via a respective peak area corresponding to the individual species. It is noted here that considerable calibration of Raman scattering strength as a function of the pressure and temperature would be required if a more accurate analysis is required. The relative abundance of CO to H_2 and CO_2 to H_2 is presented in Figure 3 as, along with the temperature variation of 160−550 °C, the pressure changes, i.e., from 1 to 5 GPa, approximately along an isochor. It is observed that the abundance of CO relative to

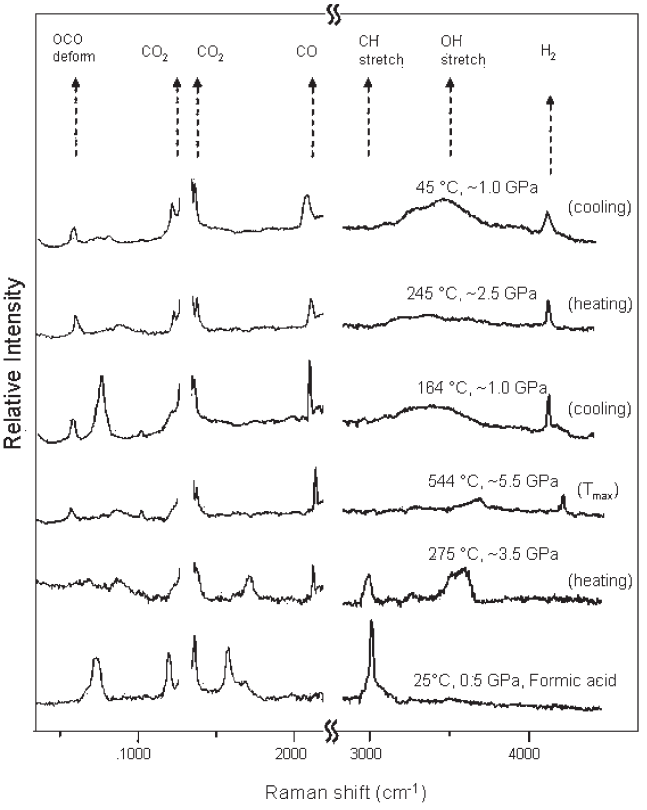

Figure 2. *In situ* Raman spectra showing the sequence of formic acid decomposition to C−H−O fluids in equilibrium through the WGS reaction at high pressures and temperature. The pure formic acid (shown at 25 °C and 0.5 GPa) undergoes thermal decomposition, as observed at 275 °C. The system was maintained at high temperature (544 °C) to complete decomposition, at which point the Raman spectra shows only the presence of H_2, CO_2, H_2O, and CO. Interestingly, CO persists to the highest temperatures and pressures, which may be due to the immiscible CO-rich composition crystallizing as a solid phase, or a possible artifact of adsorption-enhanced effects. Notably, upon a pressure increase at a given temperature, the system was observed to ultimately reach complete miscibility.

H_2 shows an apparent increase with temperature, consistent with thermodynamic expectations.[29] The relative amount of CO_2 and H_2 remains essentially constant, which is expected if facile re-equilibration across the WGS reaction follows with increasing temperature. It is not possible to obtain a reasonable estimate of the H_2O content because of the appreciable broadening and line shape changes of the Raman bands, but with mass conservation in a closed system, the H_2O content is expected to follow CO and increase relative to H_2 with temperature. Note that the trend of CO/H_2 increasing with temperature is completely opposite that observed by Morgan et al.,[29] who, contrary to thermodynamic considerations, observed CO/H_2 dropping with increased temperature. Morgan et al.[29] concluded that the apparent reduction in CO in their experiments was actually due to a progressive H_2 loss from their silica tube reactors. In the present case with the DAC experiments, H_2 loss is not observed at these temperatures and pressures over the time scale of the runs and the system could be maintained at the WGS stoichiometry for several days with repeated cycles of heating.

3.2. CO_2-H_2 Reactions in the Presence of Fe or FeO. As noted earlier, exposing transition-metal containing (e.g., stainless steel) reactors to formic-acid-derived fluids at elevated temperature and pressure changes the chemistry

(22) Brill, T. B. Geothermal vents and chemical processing: The infrared spectroscopy of hydrothermal reactions. *J. Phys. Chem. A* **2000**, *104*, 4343–4351.
(23) Goddard, J. D.; Yamaguchi, Y.; Schaefer, H. F., III The decarboxylation and dehydration reactions of monomeric formic acid. *J. Chem. Phys.* **1992**, *96*, 1158–1166.
(24) Huebner, J. S. Use of gas mixtures at low pressure to specify oxygen and other fugacities of furnice atmospheres. In *Hydrothermal Experimental Techniques*; Ulmer, G. C., Barnes, H. L., Eds.; John Wiley and Sons: New York, 1987; pp 20−60.
(25) Rice, S. F.; Steeper, R. R.; Aiken, J. D. Water density effects on homeogeneous water−gas shift reaction kinetics. *J. Phys. Chem. A* **1998**, *102*, 2673–2678.
(26) Seewald, J. S.; Zolotov, M. Y.; McCollom, T. Experimental investigation of single carbon compounds under hydrothermal conditions. *Geochim. Cosmochim. Acta* **2006**, *70*, 446–460.
(27) Chou, I. M.; Sharma, A.; Burruss, R. C.; Hemley, R. J.; Goncharov, A. F.; Stern, L. A.; Kirby, S. H. Diamond-anvil cell observation of a new methane hydrate phase in the 100-MPa pressure range. *J. Phys. Chem. A* **2001**, *105*, 4664–4668.
(28) Chou, I. M.; Sharma, A.; Burruss, R. C.; Shu, J.; Mao, H. K.; Hemley, R. J.; Goncharov, A. F.; Stern, L. A.; Kirby, S. H. Transformations in methane hydrates. *Proc. Nat. Acad. Sci. U.S.A.* **2000**, *97*, 13484–13487.
(29) Morgan, G. B., VI; Chou, I. M.; Pasteris, J. D. Speciation of experimental C−H−O fluids produced by thermal decomposition of oxalic acid dehydrate. *Geochim. Cosmochim. Acta* **1992**, *56*, 281–294.

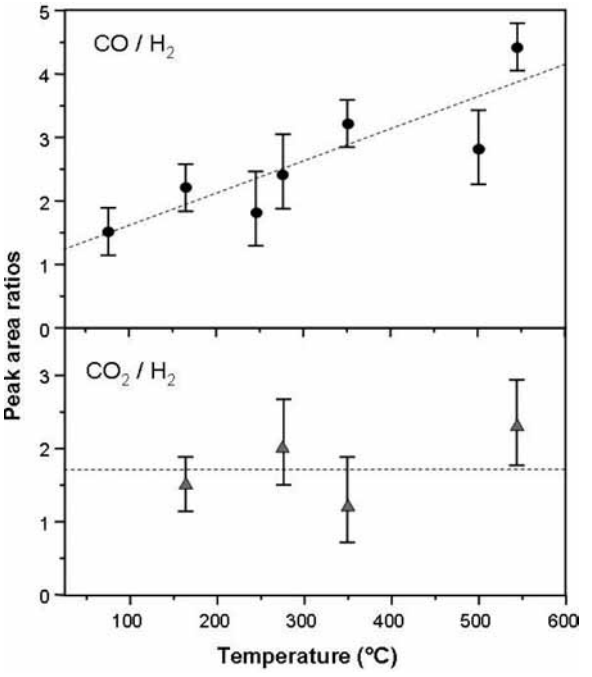

Figure 3. Plot of Raman peak area ratios of CO/H_2 and CO_2/H_2 with temperature derived by fitting Raman peaks of CO (~2100 cm^{-1}), H_2 (~4200 cm^{-1}), and CO_2 (~1370 cm^{-1}). Subsequent to the formic decomposition, the CO/H_2 ratio shows an increase with temperature, which reflected an increasing phase immiscibility. The close proximity of CO_2 peaks to the diamond peak at 1330 cm^{-1} allowed for only 4 peak area ratio determinations.

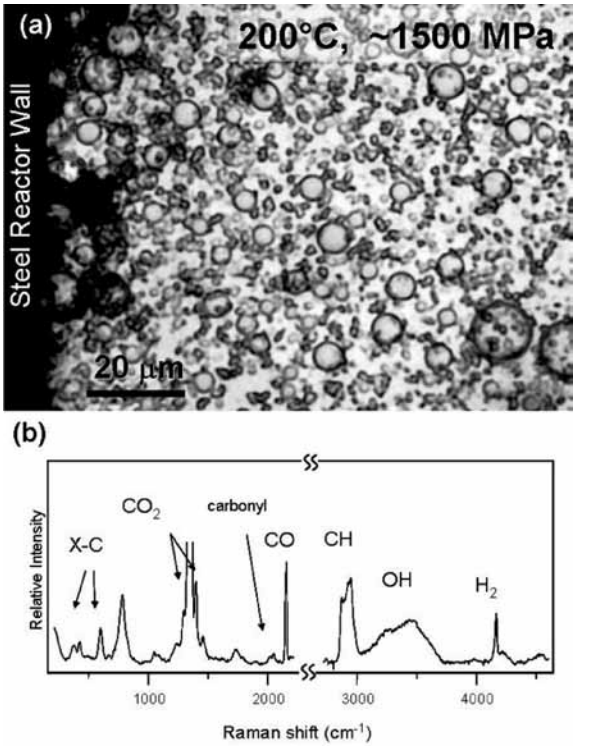

Figure 4. (a) Metal leaching at ~200 °C and 1.5 GPa, within 2–3 min from the start of the heating run with dilute formic acid (50 mol %) loaded in a stainless-steel gasket. The optical micrograph here shows extensive immiscibility of the reddish brown (CO-rich) fluid phase containing Fe, Ni, V carbonyl-type metal carbonyl complexes surrounded by the aqueous phase. Upon increasing pressure to 3 GPa, the immiscible CO-rich phase was observed to crystallize at 200 °C. This phase transformation is reversible and may play a role in sequestering the reduced carbon phase at high $P-T$ conditions. (b) *In situ* Raman spectra of the fluid phase (indicated as a "star" in the image) show strong vibration peaks for the carbonyl (~1600 cm^{-1}) along with the metal–carbon stretch in the 500 cm^{-1} range that evolved rapidly with increasing temperature and duration of heating. In longer duration heating, the CO-stretch peak reduced with further formation of the metal–carbonyl.

dramatically with the incorporation of reactor-wall-derived transition metals into the reacting system.[13,16] To explore the role of reduced metals (and metal oxide) in enhancing the formation of methane (as is observed if the metal gaskets without gold linears are used), a set of experiments starting with pure formic acid with a steel gasket or Fe/FeO nanoparticles (with a gold-lined gasket) were performed (runs 3–6 in Table 1 and Figure 1).

For reaction runs 3, 4, 5, and 6 (Table 1) at 250, 440, 360, and 440 °C (1.0, 1.5, 1.5, and 2.5 GPa, respectively), a deep orange to red color fluid phase consistent with metal carbonyl formation developed,[16] which was confirmed with the presence of fingerprint Fe–C (400–600 cm^{-1}) and the corresponding carbonyl stretch (1700–2100 cm^{-1}) peaks (Figure 4). It is noteworthy that the metal–carbonyl complex shows systematic changes in the Raman spectra, likely indicative of a compositional variation in response to shifts in the equilibrium conditions. This proposal is consistent with the observation that the carbonyl phase stability is reversible, such that changes in pressure at high temperatures correlate with changes in the abundance of the immiscible phase. The formation of these organometallic compounds is not surprising, and such species are expected to be favored at higher pressures. For example, it has been shown in reactions of FeS and aqueous formic acid that considerable $Fe(CO)_5$ and other carbonylated iron species form and the yield of these carbonylated iron species is strongly enhanced with increased pressure (from 50 to 200 MPa).[16,30,31]

In addition to the carbonylated species, abundant iron carbonate along with methane was observed, which was more readily discernible upon prolonged heating in run 5 (> 1.5 h heating at 560 °C and 3.5 GPa) (Table 1). The Fe metal-bearing system, upon prolonged heating (> 1.5 h at ~550 °C and 3.5 GPa), produced a crystalline mass of iron–carbonate (siderite) with inclusions (~5 μm) of methane-rich fluids (Figures 5 and 6). The small size of fluid inclusions (< 5 μm) made it difficult to ascertain the predominant composition of the hydrocarbon phase, although the C–H stretching band is observed to be rather broad (Figure 6). It is possible that the Raman peak broadening is due to the formation of a clathrate phase of methane within the fluid inclusions upon cooling.[27,28]

The formation of abundant transition-metal carbonyl species changes the solution chemistry considerably, pulling the fluid chemistry toward a CO- and H_2O-rich composition, reducing the activity of H_2, and presumably lowering significantly the thermodynamic driving force for methane and/or hydrocarbon formation. This chemical trend is balanced, however, by the concomitant oxidation of some of the transition metal to oxides (evident via the formation of

(30) Cody, G. D.; Boctor, N. Z.; Brandes, J. A.; Filley, T. R.; Hazen, R. M.; Yoder, H. S., Jr. Assaying the catalytic potential of transition metal sulfides for abiotic carbon fixation. *Geochim. Cosmochim. Acta* **2004**, *68*, 2158–2196.

(31) Cody, G. D.; Boctor, N. Z.; Filley, T. R.; Hazen, R. M.; Scott, J. H.; Sharma, A.; Yoder, H. S., Jr. Primordial carbonylated iron–sulfur compounds and the synthesis of pyruvate. *Science* **2000**, *289*, 1339–1341.

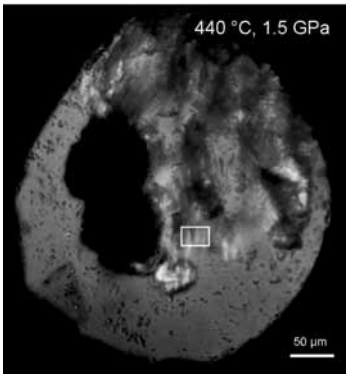

Figure 5. Microphotograph of the formic acid/Fe nanoparticle sample in the DAC under crossed-polarized light, showing the birefringent carbonate crystals at ambient temperature and high pressure (~0.8 GPa). The dark regions within the sample chamber are clusters of Fe and FeO nanoparticles, while the crystals scattered away from the carbonate and nanoparticle clusters are Fe−carbonyl-phase-immiscible from the surrounding aqueous phase. These scattered carbonyl phases are typically observed to migrate along the diamond surfaces. The drawn rectangle highlights the region shown in Figure 6 at higher magnification.

siderite) yielding an additional source of H_2. The resultant fluid composition is thus CO- (in the form of transition-metal carbonyls) and H_2-rich. Such a fluid composition is evidently highly amenable to the formation of abundant methane and hydrocarbons, indicating that kinetic barriers for the reduction of CO are removed in the presence of metal−carbonyl complexes. It is likely that the most important role of the transition-metal−carbonyl complexes is to activate H_2 by the incorporation of hydrogen into the transition-metal−carbonyl complexes.[32]

3.3. CO_2−H_2 in the Presence of Graphite. In geologic settings, C−H−O fluids typically exist in equilibrium with graphite[33−35] or diamond at extremely high pressures.[36] Thermodynamic calculations predict at high H_2 fugacity a three-phase system composed of graphite and two immiscible fluids, one CH_4-rich and the other H_2O-rich.[34] Evidence from natural settings predominantly show fluid inclusions enriched in CO_2 occasionally associated with graphite (in some cases, hydrocarbons) in and around igneous and metamorphic provinces that point to the carbonate

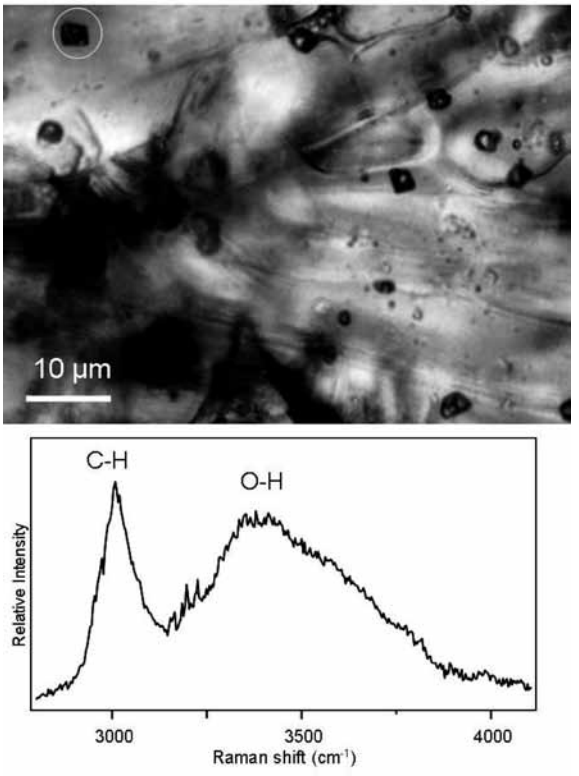

Figure 6. Close-up view of the carbonate crystals under transmitted light showing approximately 5 μm fluid inclusions containing methane or its analogues. The fluid inclusions within the carbonates are typically rhombic negative crystal shapes containing at least one fluid phase. Several scattered Fe−carbonyl phases are also seen scattered as translucent phases on the carbonate crystal surface (lower right region). The Raman spectrum shown is from the single fluid inclusion in the upper left corner of the image (highlighted with a circle, the size of which approximates the laser spot).

reduction process producing hydrocarbon at moderate to high $P-T$ conditions.[37−39] Carbon isotope data from the graphite from hydrothermal veins within high-grade metamorphic rocks show a wide dispersion of values (from −28 to −9%), suggesting mixing of reduced carbon and carbonate fluids from different sources at high $P-T$ conditions.[39] To explore whether the addition of graphite leads to the establishment of such an equilibrium assemblage, a series of experiments were performed with formic acid and graphite as the starting composition. Reactions were run at temperatures of 350−550 °C and pressures of 3−4.5 GPa, respectively (Table 1).

In these experiments, the C−H−O fluids (from formic acid) were observed to react significantly with graphite, yielding a fluid that contains abundant methane and heavier hydrocarbons, in addition to CO_2 and H_2O with minor amounts of CO and H_2 (Figure 7). At least three distinct C−H symmetric stretching peaks (~3000 cm^{-1}) were observed at high $P-T$ conditions (Figure 8), which indicates the presence of methane with additional homologues (e.g., ethane). *In situ* Raman observations indicate that the fluid at high pressures and temperatures is dominated by CO_2; a CO-containing immiscible fluid is also present, as clearly shown in Figure 7. These observations point to CO_2−H_2O−CH_4−C as the equilibrium phase assemblage with increased methane formation with the presence of graphite (Figure 9). Whereas the potential of transition metals to lower kinetic barriers for methane formation (presumably

(32) Cotton, F. A.; Wilkinson, G. *Advanced Inorganic Chemistry*; John Wiley and Sons: New York, 1988.
(33) French, B. M. Some geological implications of equilibrium between graphite and a C−H−O gas at high temperatures and pressures. *Rev. Geophys.* **1966**, *4*, 223–253.
(34) Holloway, J. R. Graphite−CH_4−H_2O−CO_2 equilibria at low-grade metamorphic conditions. *Geology* **1984**, *12*, 455–458.
(35) Rumble, D.; Duke, E. F.; Hoering, T. C. Hydrothermal graphite in New Hampshire: Evidence of carbon mobility during regional metamorphism. *Geology* **1986**, *14*, 452–455.
(36) Eggler, D. H.; Baker, D. R. Reduced volatiles in the system C−O−H: Implications to mantle melting, fluid formation, and diamond genesis. In *High-Pressure Research in Geophysics*; Akimoto, S., Manghnani, M. H., Eds.; Advances in Earth and Planetary Sciences: Tokyo, Japan, 1982; Vol. 2, pp 237−250.
(37) Beeskow, B.; Treloar, P. J.; Rankin, A. H.; Vennemann, T. W.; Spangenberg, J. A reassessment of models for hydrocarbon generation in the Khibiny nepheline syenite complex Kola Peninsula, Russia. *Lithos* **2006**, *91*, 1–12.
(38) Potter, J.; Rankin, A. H.; Treloar, P. J. Abiogenic Fischer−Tropsch synthesis of hydrocarbons in alkaline igneous rocks; fluid inclusion, textural and isotopic evidence from the Lovozero complex, N.W. Russia. *Lithos* **2004**, *75*, 311–330.
(39) Rumble, D.; Hoering, T. C. Carbon isotope geochemistry of graphite vein deposits from New Hampshire, U.S.A. *Geochim. Cosmochim. Acta* **1986**, *50*, 1239–1247.

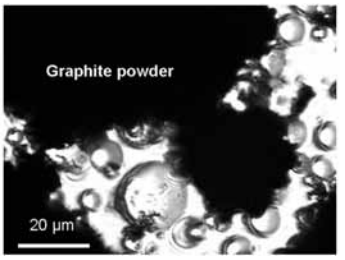

Figure 7. Microphotograph of the formic acid−graphite sample after quench from high $P-T$ clearly shows phase immiscibility. The dark gray material is graphite, while the "bubbles" of CO_2 and also CO are surrounded with the aqueous phase. The continuous motion of the fluids along with rapid mixing of opaque graphite made it difficult to ascertain the proportion of CO to CO_2 phases within the system.

through H_2 activation) are reasonably well-understood, the mechanism by which graphite would enhance methane formation from C−H−O fluids remains ambiguous.

3.4. Graphite−Hydrogen. It is possible that in the formic acid−graphite experiments methane formation occurred as a consequence of the direct hydrogenation of graphite. To test this possibility, two sets of experiments (runs 10 and 11 in Table 1) were performed with graphite and H_2. These experiments required high-pressure gas loading (see the Experimental Section). Anticipating that such a reaction would be sluggish, laser heating was used to heat the sample to temperatures on the order of 1500 °C over a short duration (10−15 s heating) and a longer duration (~2 min heating). Raman spectroscopy performed after heating revealed the presence of a strong hydrocarbon signal (methane and higher hydrocarbons) along with H_2 (~5−10 wt % based on peak intensity) (Figure 10). The direct hydrogenation of graphite to methane, i.e.,

$$\mathrm{C\ (graphite)} + 2\mathrm{H_2} \rightarrow \mathrm{CH_4} \qquad (1)$$

and even higher hydrocarbons is thus facile under these conditions.

In addition to methane, ethane and higher hydrocarbons were also observed in the Raman spectrum for the longer duration heating run with several weaker C−H stretching peaks at different frequencies relative to methane (Figure 10). The longer duration heating run also shows a possible weak C−H peak close to 3070 cm^{-1}, which may indicate the formation of an alkene (e.g., ethylene). Specific compound identification will require supplemental techniques, such as gas chromatography of samples recovered from the DAC.[16] The formation of these other hydrocarbons may be a result of the simultaneous backward reaction (eq 2) toward eventual methane decomposition into C_2 or higher hydrocarbons because of local reduction of the H_2 concentration as a result of diffusion of H_2 away from the laser-heated spot along the $P-T$ gradients induced by the spatially localized laser heating. Such secondary reactions are therefore variations of the following dehydrogenation reaction:

$$x\mathrm{CH_4} \rightarrow \mathrm{C}_x\mathrm{H}_y + \mathrm{H_2} \rightarrow \mathrm{C} + \mathrm{H_2} \qquad (2)$$

3.5. Carbonate Reduction Series ($CaCO_3$−Fe_xO−H_2O). These experiments were aimed at determining whether reactions of FeO with H_2O and $CaCO_3$ produce a sufficiently reduced carbon bearing fluid to favor thermodynamically the formation of methane and higher hydrocarbons.

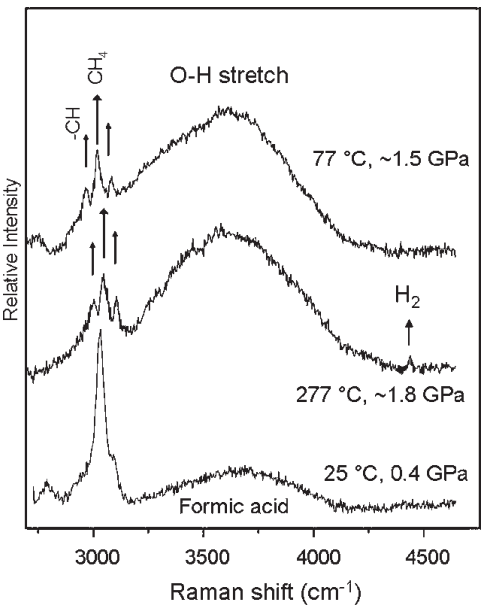

Figure 8. Raman spectra of the formic acid−graphite sample heated to ~450 °C show at least three different C−H stretching modes (2850−2950 cm^{-1}), which indicate the presence of methane and other analogues. On the basis of the peak shift, higher order alkanes (such as ethane) could be a possible phase with its symmetric and asymmetric C−H stretch on either side of the more intense methane peak. The spectra were collected during the cooling cycle.

The previous DAC experiments of Scott et al.[12] explored the reaction

$$12\mathrm{FeO} + \mathrm{CaCO_3} + 2\mathrm{H_2O} \rightarrow 4\mathrm{Fe_3O_4} + \mathrm{CH_4} + \mathrm{CaO} \qquad (3)$$

H_2 was derived from the reaction of H_2O with FeO forming magnetite; CO_2 was derived from the thermal decarbonation of $CaCO_3$, while methane was produced though reactions within the resultant C−H−O fluid at temperatures of 500 and 1500 °C and pressures between 5 and 11 GPa. The results indicated that, at reaction conditions of 550 °C and 5.5 GPa, the kinetic barrier for methane formation directly from C−H−O fluids remains substantial and no methane is detected.[12] This observation suggests that magnetite may have acted catalytically to aid in the formation of methane. In these experiments, however, steel gaskets with no Au linears were employed.[12] As discussed above, reduced iron reacts with C−H−O fluids, producing carbonylated transition-metal complexes that afford facile CO reduction to methane and other hydrocarbons.

To explore this reaction further, a series of experiments using FeO powder, $CaCO_3$, and water were performed with a steel gasket (run 13), with a gold linear and Fe and Ni nanoparticles (run 12), and with a gold linear only (runs 14 and 15) (Figure 11). Reaction of FeO, $CaCO_3$, and H_2O using a steel gasket yields a considerable quantity of methane and other hydrocarbons, iron carbonyl, and $FeCO_3$ along with CO_2, CO, H_2, and H_2O fluid (Figure 12). These results largely replicate those of the previous study; however, here, we also document the presence of carbonylated iron in these solutions.

Reactions using a gold linear isolating the gasket fluid but adding Fe and Ni nanoparticles to the FeO, $CaCO_3$, and H_2O system at 550 °C and 7.0 GPa (run 12) also yield considerable methane and other hydrocarbons (Figure 12). This is consistent to what is observed with simple C−H−O

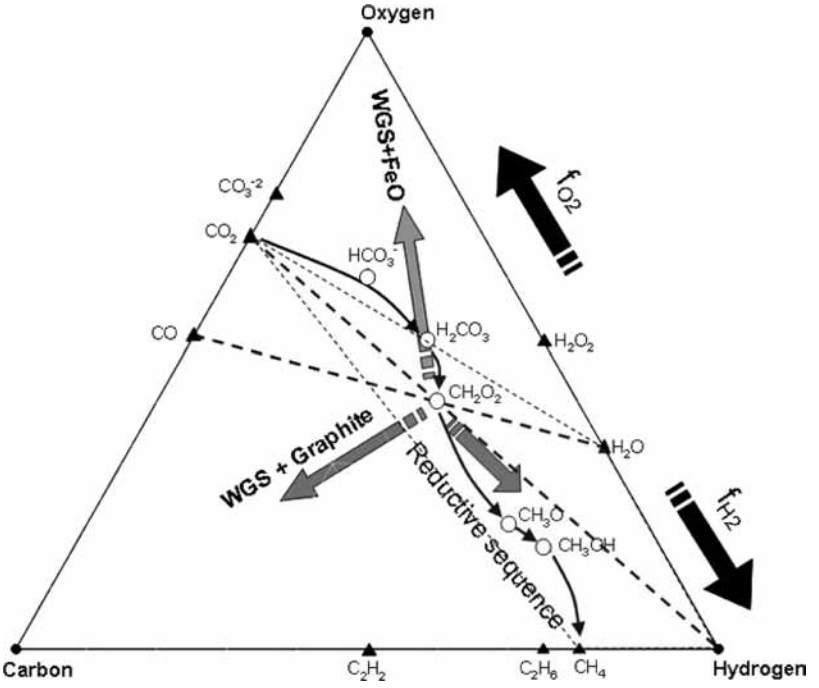

Figure 9. Reduction sequence, shown by arrows, in the C−H−O system that includes C1 phases (CO_2, carbonic acid, formic acid, formaldehyde, methanol, and methane). Each of the reduction steps involve some combination of hydrogenation and dehydration, resulting in added hydrogen and loss of total oxygen. The WGS reaction is shown with dashed lines intersecting at formic acid. Also shown (gray arrows) are the general direction of compositional shifts from the WGS (formic acid) reaction for the bulk system in experimental excursions, which have been investigated for hydrocarbon synthesis in this study. When the bulk chemistry is changed from the HCOOH composition, the effective variations in the fugacities (f_{O_2} and f_{H_2}) can be achieved.

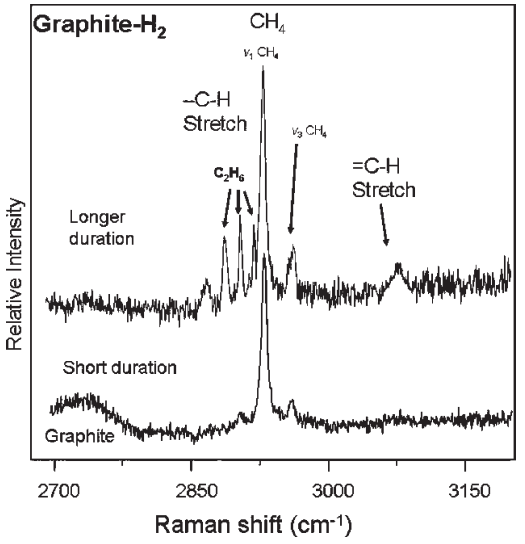

Figure 10. Raman spectra of the graphite−hydrogen reaction at high pressure and temperature. The pressure, measured at room temperature, was 2 GPa. During laser heating (>1000 °C), the pressure was likely much higher. The higher resolution spectrum in the C−H stretching region for a short (~10 s) heating shows a strong methane peak (2925 cm^{-1}). The broad peak around 2730 cm^{-1} is from graphite. The longer (~30 s) duration laser heating shows a much more complex pattern of peaks in the C−H stretch region. The relative shifts from the main methane peak (2925 cm^{-1}) with multiple C−H peaks on either side likely indicate higher order alkanes (−C−H symmetric stretching at ~2900 cm^{-1}) as well as an aromatic with a peak at 3075 cm^{-1}.

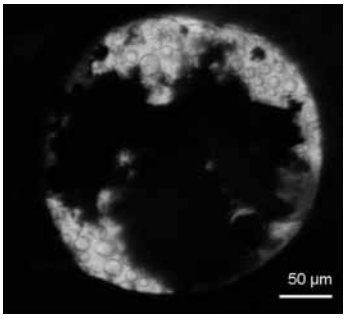

Figure 11. Micrograph of the sample at high temperature and pressures in a gold-lined reactor shows the presence of an immiscible CO_2- and CO-rich fluid phase associated within the aqueous rich phase. This image was taken at 160 °C and 1.5 GPa. The dark phase is a mixture of FeO and $CaCO_3$, while the predominantly CO_2-rich (along with CO) phase occurs as immiscible "bubbles".

fluids derived from formic acid. Both of these reactions unambiguously confirm that carbonate−water−iron reactions yield a C−H−O fluid capable of forming methane. The Au-lined runs 14 and 15 (Table 1) reacted at 350 °C and 4.0 GPa and 620 °C and 6.5 GPa, respectively, for >2 h, yielding very little methane, in comparison to those containing transition metals (runs 12 and 13). Previously, we showed that FeO reacting with formic-acid-derived C−H−O fluids with gold-lined gaskets (run 5 in Table 1) is capable of generating methane; therefore, the lack of significant methane in the present experiment is puzzling and likely reflects the difficulty of achieving the optimum initial stoichiometry to achieve high quantities of methane and other hydrocarbons.

4. Concluding Remarks

We have carried out *in situ* observations on C−H−O fluid reactions at pressures and temperatures relevant to the Earth's lower crust and upper mantle. Incorporating a number of

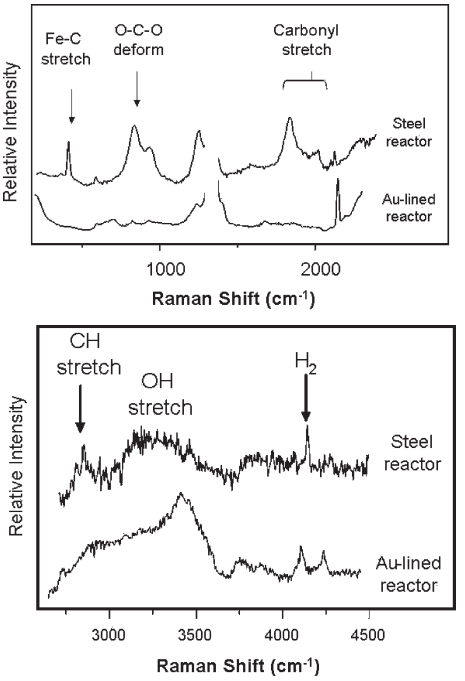

Figure 12. *In situ* Raman spectra of run products. The top spectra shows the carbonate reduction run in a stainless-steel gasket, while the bottom spectra is the same run in a Au-lined gasket. Note that, in both runs, there is a significant amount of CO (~2100 cm^{-1}), although in the stainless-steel run, it has combined with the transition metals to form complexes that are characterized by multiple peaks of CO, coupled with peaks from the metal−carbon (M−CO) stretch near ~400 cm^{-1}. The duel peaks of hydrogen in the Au-reactor spectra are likely a consequence of H_2 bearing clathrate formation that formed upon cooling, which displaces the hydrogen vibron from the fluid value.[42]

compositions and a wide range of $P-T$ conditions as would be encountered along a subduction geotherm, insights into the formation of intermediates, and the role of transition metals and possible pathways toward hydrocarbon synthesis have been revealed. The results shed light on earlier high-pressure studies that defined thermodynamic feasibility of hydrocarbon formation but presented questions about kinetic barriers to methanogensis.

The compositional variation of formic-acid-derived C−H−O fluids examined in this study reflect corresponding variations in f_{H_2}, f_{CO_2}, f_{CO}, f_{H_2O}, and C_{total}, which are strongly related to the oxidation states of added transition metals and thereby provide a compositional map of the methane-forming region within the C−H−O system. The addition of transition metals to the formic-acid-derived C−H−O fluids shifts the solution chemistry by partitioning significant quantities of CO into metal carbonyl complexes, which evidently strongly favor methane and hydrocarbon synthesis. The addition of graphite yielded the greatest amount of methane, likely because of facile graphite hydrogenation rather than through graphite-enhanced CO_2 (or CO) reduction.

The reduction of CO_2 to form methane is often mediated via $CO-H_2$ bearing heterogeneous pathways coupled with the oxidation of metal/metal oxide phases that define the redox potential of the system. A recent report[40] using a similar reactant composition at higher temperatures (~600 °C and 6 GPa) indicated the formation of abundant hydrocarbons, but the detection of hydrogen was not reported. In light of the data presented above, the observation of H_2 provided an important contrast because the abundance (high f_{H_2}) is essential for synthesis and stability of hydrocarbons.

These high $P-T$ experiments thus demonstrate that, under lower crust and upper mantle conditions, f_{H_2} is the critical variable for hydrocarbon formation. Direct CO_2 reduction, even with relatively high f_{H_2} to methane, is evidently kinetically inhibited even at high temperatures but is facile in the presence of transition-metal complexes. Improved thermochemical characterization of these metal carbonyl complexes would be useful for assessing the full potential for hydrocarbon synthesis at these high $P-T$ conditions. The formation of metal carbonyl complexes alter not only the chemical equilibrium but act as a temporary sink for carbon (and likely hydrogen) on route to methanogenesis. Furthermore, the end product of this reaction, methane, may or may not leave a clear signature of the involvement of transition-metal carbonyls, and if mantle-derived methane is discovered to be more widespread than currently considered, then the conclusion that CO_2 is the primary carbon-volatile species in the Earth's mantle may warrant re-evaluation.[41] From this and earlier studies, it is concluded that the critical variable governing methanogensis is f_{H_2}. The fact that hydrogen is formed from the oxidation of both reduced and ferrous iron by water under all conditions strongly suggests that it is likely that, in deep earth geologic systems, some methane generation is inevitable.

Acknowledgment. We thank M. Somayazulu, C. S. Zha, R. Chellappa, and A. F. Goncharov for help with the experiments and L. Goncalves-Ferreira, S. G. Bergman, H. F. Detlef, D. Foustoukos, D. Sverjensky, S. Gramsch, Chr. Jonsson, C. Jonsson, and V. V. Struzkin for discussions and comments on the manuscript. This work was funded in part by a research grant from Shell International E&P, Inc. and Stichting Shell Research, with additional support from NSF-EAR, DOE/NNSA (CDAC), Carnegie Institution of Washington, and the Balzan Foundation.

(40) Chen, J. Y.; Lin, L. J.; Dong, J. P.; Zeng, H. F.; Liu, G. Y. Methane formation from $CaCO_3$ reduction catalyzed by high pressure. *Chin. Chem. Lett.* **2008**, *19*, 475–478.

(41) Sleep, N. H.; Zahnle, K. Carbon dioxide cycling and implications for climate on ancient Earth. *J. Geophys. Res.* **2001**, *106*, 1373–1399.

(42) Mao, W. L.; Mao, H. K.; Goncharov, A. F.; Struzhkin, V. V.; Guo, Q.; Hu, J.; Shu, J.; Hemley, R. J.; Somayazulu, M.; Zhao, Y. Hydrogen clusters in clathrate hydrate. *Science* **2002**, *297*, 2247–2249.